



CHORUS

This is the accepted manuscript made available via CHORUS. The article has been published as:

Dislocation-Pairing Transitions in Hot Grain Boundaries

David L. Olmsted, Dorel Buta, Ari Adland, Stephen M. Foiles, Mark Asta, and Alain Karma

Phys. Rev. Lett. **106**, 046101 — Published 24 January 2011

DOI: [10.1103/PhysRevLett.106.046101](https://doi.org/10.1103/PhysRevLett.106.046101)

Dislocation-Pairing Transitions in Hot Grain Boundaries

David L. Olmsted,¹ Dorel Buta,² Ari Adland,³ Stephen M. Foiles,⁴ Mark Asta,^{1,2,5} and Alain Karma³

¹*Department of Materials Science and Engineering, University of California, Berkeley, CA*

²*Department of Chemical Engineering and Materials Science, University of California, Davis, CA*

³*Department of Physics and Center for Interdisciplinary Research on Complex Systems, Northeastern University, Boston, MA*

⁴*Computational Materials Science and Engineering Department, Sandia National Laboratories, Albuquerque, NM*

⁵*Materials Science Division, Lawrence Berkeley National Laboratory, Berkeley, CA*

We report the finding of a novel grain-boundary structural phase transition in both molecular-dynamics and phase-field-crystal simulations of classical models of bcc Fe. This transition is characterized by pairing of individual dislocations with mixed screw/edge components. We demonstrate that this type of transition is driven by a combination of factors including elastic-softening, core interaction and core disordering. At high homologous temperatures the occurrence of this transition is shown to prevent premelting at misorientation angles where it would otherwise be expected.

PACS numbers:

The properties of polycrystalline materials are often strongly influenced by processes occurring at internal grain-boundaries (GBs). These processes themselves are known to be strongly influenced by the details of GB interfacial atomic structure. Due to its broad importance, theoretical, computational and experimental studies of GB structure have been pursued for several decades [1]. These studies have established that GB structures at low temperatures (T) are generally characterized by multiple metastable energy minima, corresponding, for example, to different numbers of atoms and relative displacements of the grains [1–3]. At high T , GB structures can be even more complex, as different metastable minima can be sampled through thermal fluctuations, and these interfaces can undergo a variety of phase transitions involving, e.g., defaceting and roughening [4, 5], premelting [6], and solute-driven structural transformations [7]. This high- T behavior can have important consequences for properties relevant to materials processing, including GB mobility [5, 8] and shear strength [9, 10].

From a fundamental viewpoint, GB structures are generally difficult to predict theoretically except in certain limits. One important limit is that of small misorientation angle (θ) between crystal grains where a GB consists of an array of well-separated dislocations interacting through the long-range elastic field. In a pioneering analysis, Read and Shockley (RS) derived from this picture a theoretical expression for the GB energy (γ_{GB}) [11–13]

$$\gamma_{\text{GB}} = E_0\theta(A - \ln\theta). \quad (1)$$

where $-E_0\theta \ln\theta \equiv E_E$ is the dominant elastic contribution to the energy of the array of GB dislocations, while $E_0A\theta \equiv E_C$ accounts for core effects and subdominant elastic contributions. In this Letter we show how an interplay of E_C and E_E can lead to a novel GB phase transition involving a change in dislocation character.

Specifically, we use molecular-dynamics (MD) and phase-field-crystal (PFC) simulations to explore the structure of high- T [100] symmetric tilt GBs for clas-

sical models of body-centered-cubic (bcc) Fe, over a wide range of θ . This study reveals the existence of a GB structural transition, illustrated in Fig. 1(a) and (b), involving pairing of GB dislocations with mixed screw/edge character to form pure edge dislocations. At high T the pairing transition tends to prevent the formation of a uniform thin liquid-like layer, which is the hallmark of GB premelting. We develop a theoretical interpretation of this transition within the framework of Eq. (1), which sheds light on its physical origin and provides a basis for predicting its occurrence in other crystal structures. For example, we explain the observation of pairing of edge dislocations in a recent PFC study of two-dimensional

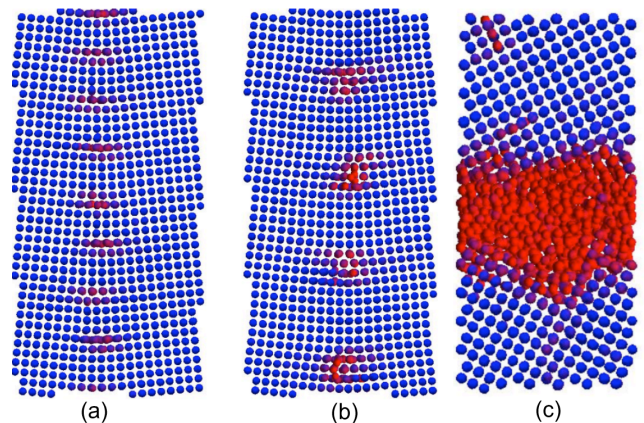


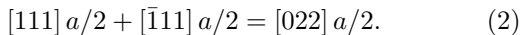
FIG. 1: MD snapshots of lower (a and b) and higher (c) angle [100] symmetric tilt GBs close to the melting temperature in bcc Fe. The boundary plane is vertical in (a and b) and horizontal in (c). Panel (a)((b)) shows the low (high) temperature configuration for a [100](0 9 11) GB heated (cooled) to $T=1300$ K. Panel (c) shows a [100](013) GB at 5 K below melting. Atomic positions have been time averaged, and colored according to the value of a local structural order parameter [14] (see supplemental material [15]). Red (blue) atoms have disordered (ordered) local atomic environments. In (a) the atoms away from the boundary on one side are further from the viewer by half the interplanar distance [15].

hexagonal crystals [16].

In the MD simulations we considered the classical potential for bcc Fe given in Ref. [17]. We begin by identifying the low-energy, zero-temperature GB structures as a function of θ , employing the minimization procedure described in [15]. For θ lower than $\theta_c \approx 21^\circ$, the low-energy structures are of the type illustrated in Fig. 1(a), composed of “unpaired” GB dislocations with mixed edge/screw character and Burgers vectors that alternate between $\mathbf{b} = [111]a/2$ and $\mathbf{b} = [\bar{1}\bar{1}\bar{1}]a/2$ along the GB length. At higher θ the stable structures are of the type shown in Fig. 1(b), composed of “paired” dislocations that are purely edge in character, with $\mathbf{b} = [022]a/2$. The zero-temperature energies for these two structures are plotted in Fig. 2(b), and are observed to cross at θ_c .

For θ below θ_c we observe a thermally-induced transformation from the unpaired to the paired state upon heating in MD simulations. In Fig. 2(a) the solid up triangles plot the values of T at which the transformation between the (low- T) unpaired structure and (high- T) paired structure are observed in these MD heating runs (an MD animation of the observed transition can be found in [15]). The solid down triangle in Fig. 2(a), for $\theta = 11.4^\circ$, indicates the temperature at which the paired structure was observed to transform back to the unpaired structure in MD cooling runs starting from high T . This observation establishes the reversible nature of the pairing transition, and also highlights the strong hysteresis of the transition in the MD simulations. For the other θ values considered unpairing was not observed on cooling, presumably due to sluggish kinetics.

The thermally-induced structural transition observed in the MD simulations corresponds to a coalescence of GB dislocations according to the reaction:



To understand the driving force for this transition we begin by using Eq. (1) and explore predictions based solely on elastic softening at high temperature. Specifically, we investigate whether the T dependence of E_0 is sufficient to stabilize the paired instead of the unpaired structure at high T . For the observed dislocations the elastic prefactors E_0 in Eq. (1) are [11, 12]:

$$E_0 = \frac{b}{2}\tau_{\text{edge}}^{(0)} \quad (3)$$

$$\tau_{\text{edge}}^{(0)} = \frac{1}{2\pi}(c_{11} + c_{12}) \left[\frac{c_{44}(c_{11} - c_{12})}{c_{11}(c_{11} + c_{12} + 2c_{44})} \right]^{1/2} \quad (4)$$

for the $[022]a/2$ pure edge dislocations, and

$$E_0 = \frac{b}{2} \left(\frac{3}{2} \right)^{1/2} \left(\frac{2}{3}\tau_{\text{edge}}^{(0)} + \frac{1}{3}\tau_{\text{screw}}^{(0)} \right) \quad (5)$$

$$\tau_{\text{screw}}^{(0)} = \frac{1}{2\pi}c_{44}, \quad (6)$$

for the alternating $[111]a/2$ and $[\bar{1}\bar{1}\bar{1}]a/2$ dislocations, where c_{ij} are the elastic moduli and b is the magnitude of the relevant Burgers vector. Using these expressions together with $c_{ij}(T)$ values calculated from $T = 0$ K to the melting point (T_M) by MD [15], the elastic prefactor is always larger for paired than unpaired structures. The ratios $E_0^{\text{paired}}(T)/E_0^{\text{unpaired}}(T)$ range from 1.3 at $T = 0$ K to 1.14 at T_M . Thus pairing would not be favorable from consideration of E_E alone. Hence E_C , which reflects core effects and subdominant elastic contributions, must favor the paired state relative to the unpaired state.

In analyzing E_C we note that previous experimental and theoretical work [12, 18, 19] suggest that the parameter A in Eq. (1) is unlikely to be constant over the range of θ studied here. We therefore proceed by allowing A to be a function of θ :

$$\gamma_{\text{GB}}(T) \approx E_0(T)\theta[A(\theta) - \ln\theta]. \quad (7)$$

For fixed θ , Eq. (7) then gives:

$$\gamma_{\text{GB}}(T) \approx \frac{E_0(T)}{E_0(T=0)}\gamma_{\text{GB}}(T=0). \quad (8)$$

From the computed zero-temperature GB energies ($\gamma_{\text{GB}}(T=0)$) for both paired and unpaired structures plotted in Fig. 2(b), we use Eq. (8) to predict the pairing transition temperature at which the two structures have equal free-energies. It should be emphasized that Eq. (8) predicts a pairing transition because the T dependence of the c_{ij} that determine E_0 through Eqs. (3)-(6) is such that E_0 decreases more rapidly for the paired structure with increasing temperature than for the unpaired structure. In particular, the ratios c_{11}/c_{44} and c_{12}/c_{44} are strongly T dependent for the Fe potential used here [15]. Note that by using the MD-calculated values of $\gamma_{\text{GB}}(T=0)$ in Eq. (8), we account for the changes in γ_{GB} arising from the θ dependence of A [15].

The results in Fig. 2(a) show that the transition temperature predicted by Eq. (8) with $E_0(T)$ from Eqs. (3)-(6) agrees remarkably well with the temperature at which pairing is observed in MD heating simulations. The pairing transition temperature increases with decreasing θ , consistent with the predictions of Eq. (8) and the expectation that the transition would not occur for very low θ where E_E is dominant. That E_C favors the paired state is clearly seen from the fact that the paired structure occurs even at $T = 0$ K for θ above $\theta_c \approx 20^\circ$.

It is important to emphasize that the pairing transition shows strong hysteresis in the MD simulations, with the homologous temperature where pairing was observed for the $\theta=11.4^\circ$ GB being 0.9, and the unpairing on cooling being 0.6. The pairing transition temperatures predicted by Eq. (8) are essentially equal to the upper bounds for the pairing transition in MD. The temperatures at which the paired and unpaired structures have equal free energies could be smaller than predicted by Eq. (8) (i.e., with

a homologous temperature between 0.6 and 0.9 for the $\theta=11.4^\circ$ GB). However, we cannot determine the difference between the upper bound and true transition temperatures from the MD simulations. We expect that any such difference would primarily be due to an effect neglected in Eqs. 7 and 8: additional temperature dependence of E_C arising from a T dependence of A . Physically, such a T dependence can arise from disordering of the dislocation cores, as we discuss next.

To gain further insights into the driving forces underlying the pairing transition we made use of a PFC model [20] that favors bcc ordering in three dimensions, with model parameters previously determined for Fe with input from MD [21]. We observe for this PFC model a qualitatively identical hysteretic pairing transition as in MD, characterized by Eq. (2), as shown in Fig. 3. A crucial difference from the MD, however, is that the ratios c_{11}/c_{44} and c_{12}/c_{44} are nearly independent of temperature in the PFC model over the entire hysteresis range (the variation being on the order of a percent), even though the magnitudes of the individual c_{ij} do decrease with increasing T . Consequently, Eq. (8) is unable to predict the observed pairing transition in the PFC model. Within the framework of Eq. (7), the PFC transition can only be explained through an explicit temperature dependence of A ; the A parameter must be lower at high T for the paired relative to the unpaired structure, presumably due to the more extended localized core disordering seen in Fig. 3 (a similar difference in the extent of core disordering in the paired and unpaired structures is also seen in MD in Fig. 1). As can be seen in Fig. 2, the transition temperature extracted from direct computations of the GB free energies in the PFC model is much closer to the upper

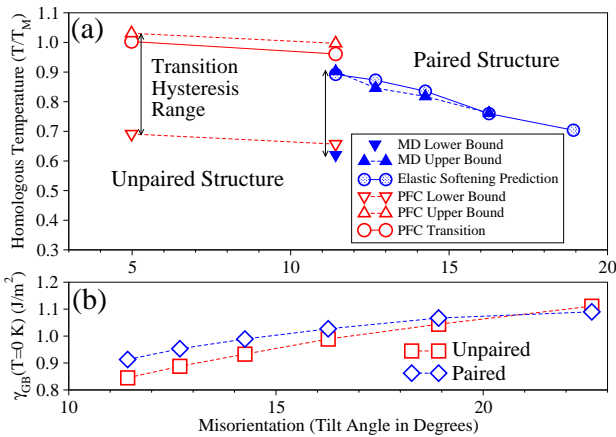


FIG. 2: (Color online) (a) Upper and lower bounds for the pairing transition temperature obtained in MD are plotted by filled up and down triangles, respectively. Predictions for the transition temperature based on an elastic softening correction to the calculated zero-temperature GB energies (shown in (b)) are plotted with shaded circles. Predictions of PFC calculations are plotted with open symbols.

than the lower bound of the hysteresis range. If the same holds true in MD, the effect of differential reduction in γ_{GB} with T arising from core disordering between the paired and unpaired structures would be a smaller effect than the T -dependence of the c_{ij} ratios, since the latter already accounts rather well for the values of the upper bound of the hysteresis range in MD.

The understanding of the factors underlying the pairing transition derived from MD and PFC allows us to conclude that it can be generally driven by elastic softening, core interactions, and core disordering, with the relative importance of each effect being system dependent. It also allows us to explain the previous observation of pairing of pure edge dislocations in PFC simulations of 2D hexagonal bicrystals [16] as being likely due to core disordering, since there the unpaired structure is always favored over the paired one in the limit of vanishing misorientation from consideration of E_E alone. Pairing in those 2D simulations was observed for symmetric tilt boundaries where each crystal is rotated $\pm\theta/2$ from a closed packed plane and $E_0^{\text{paired}}/E_0^{\text{unpaired}} = 3/2$ independent of T [15].

To give an example of the potential importance of the pairing transition found in this study, we consider the thermodynamic competition between the different structures illustrated in Fig. 1. Consider first the high-angle ($\theta = 36.9^\circ$) GB in Fig. 1(c), which features a “premelted” interfacial layer at T close to T_M (shown at 5 K below T_M in this case). Such interfacial premelting is expected to occur when:

$$\gamma_{GB}(T_M)/2\gamma_{SL} > 1 \quad (9)$$

where γ_{SL} denotes the excess free energy of the solid-liquid interface, and $\gamma_{GB}(T_M)$ is the free energy of a non-premelted GB at the melting point. Importantly, $\gamma_{GB}(T_M)$ can be significantly lower than the correspond-

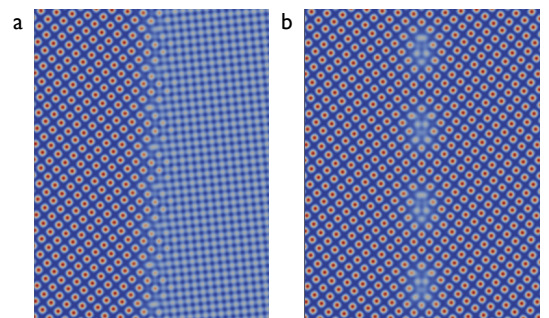


FIG. 3: Unpaired (a) and paired (b) GB structures from PFC simulations for Fe at 1720 K for the $[100](0\ 9\ 11)$ tilt GB ($\theta = 11.4^\circ$). Planar sections of the three-dimensional density field in (100) planes are shown with density peaks (red) corresponding to atomic positions; in (a), this section is in a plane (midway between two planes) of atoms in the left (right) grain due to the screw component of unpaired dislocations. (See the caption of Fig. 1(a) and [15].)

ing value at $T = 0$ K. Previous work [16, 22] suggests that reasonable estimates for $\gamma_{\text{GB}}(T_M)$ can be obtained using an elastic-softening correction, involving multiplication of $\gamma_{\text{GB}}(T = 0\text{K})$ by the ratio of an appropriate product of lattice constant and elastic moduli at T_M and $T = 0\text{K}$. In this work we use Eq. (8) to implement this correction. The resulting values provide an estimate of $\gamma_{\text{GB}}(T_M)$ for a GB with the ordered, zero-temperature interfacial structure preserved up to T_M .

A comparison of predicted and observed GBs that pre-melt is shown in Fig. 4, where GBs that do not show pre-melting in MD are indicated by circles. For Fe boundaries with normals near [001] (θ near 90°), the critical θ for pre-melting seen in MD agrees very well with the prediction based on Eq. (9). For the boundaries with normals near [011] (small θ), non-premelted states are stable to values of $\gamma_{\text{GB}}(T_M)/2\gamma_{\text{SL}}$ significantly greater than one, based on the elastic-softening estimate of $\gamma_{\text{GB}}(T_M)$. In this case the dislocation-pairing transition lowers the free energy of the non-premelted state of the GB below the value predicted by the elastic-softening correction. The pairing transition is thus responsible for the observed enhanced stability of the non-premelted states at higher θ .

The effects on GB properties resulting from pre-melting have been discussed extensively, and include enhanced GB diffusion rates [23–25], and pronounced reductions in the resistance to shear [9, 10]. The fact that the pairing transition delays pre-melting to higher misorientation angles is thus potentially significant. For example, the ordered regions of the GB between the disordered cores that are present in the paired state (see Fig. 1) should

lead to enhanced strength at higher homologous temperatures relative to a premelted boundary. Further work is warranted to understand the effects of the pairing transition on GB properties more generally, and the present work provides guidelines for the conditions under which this transition is expected to occur.

This work was supported by the US Department of Energy (DOE), Office of Basic Energy Sciences, contracts DE-AC02-05CH11231, DE-FG02-06ER46282, and DE-FG02-07ER46400. Sandia is a multiprogram laboratory operated by Sandia Corporation, a Lockheed Martin Company, for the DOE's National Nuclear Security Administration under contract DE-AC04-94AL85000. We acknowledge support from the DOE Computational Materials Science Network program, and the National Research Scientific Computing Center (DOE Office of Science contract DE-AC02-05CH11231).

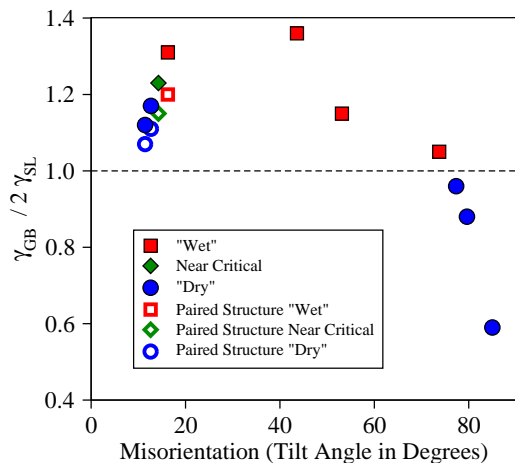


FIG. 4: (Color online). The vertical axis plots $\gamma_{\text{GB}}/2\gamma_{\text{SL}}$, where γ_{GB} is estimated based on the elastic-softening correction described in the text. GBs above (below) the horizontal line are predicted to pre-melt (not to pre-melt). Predictions are compared to MD results, where squares and circles represent GBs that are observed to pre-melt or not in MD, respectively; diamonds correspond to GBs for which pre-melting behavior could not be unambiguously determined.

-
- [1] A. P. Sutton and R. W. Balluffi, *Interfaces in crystalline materials* (Oxford: Clarendon Press, New York, 1995).
- [2] S. von Althaus, P. D. Haynes, K. Kaski, and A. P. Sutton, *Phys. Rev. Lett.* **96**, 055505 (2006).
- [3] A. L. S. Chua, N. A. Benedek, L. Chen, M. W. Finnis, and A. P. Sutton, *Nature Mater.* **9**, 418 (2010).
- [4] I. Daruka and J. C. Hamilton, *Phys. Rev. Lett.* **92**, 246105 (2004).
- [5] D. L. Olmsted, S. M. Foiles, and E. A. Holm, *Scripta Mater.* **57**, 1161 (2007).
- [6] R. Kikuchi and J. W. Cahn, *Phys. Rev. B* **21**, 1893 (1980).
- [7] D. Udler and D. N. Seidman, *Phys. Rev. Lett.* **77**, 3379 (1996).
- [8] E. A. Holm and S. M. Foiles, *Science* **328**, 1138 (2010).
- [9] J. Q. Broughton and G. H. Gilmer, *Modelling Simul. Mater. Sci. and Eng.* **6**, 87 (1998).
- [10] J. W. Cahn, Y. Mishin, and A. Suzuki, *Acta Mater.* **54**, 4953 (2006).
- [11] J. P. Hirth and J. Lothe, *Theory of dislocations* (Wiley, New York, 1982), 2nd ed.
- [12] W. T. Read, *Dislocations in crystals* (McGraw-Hill, New York, 1953).
- [13] W. T. Read and W. Shockley, *Phys. Rev.* **78**, 275 (1950).
- [14] J. R. Morris, *Phys. Rev. B* **66**, 144104 (2002).
- [15] See EPAPS Document No. for additional information. For more information on EPAPS, see <http://www.aip.org/pubservs/epaps.html>.
- [16] J. Mellenthin, A. Karma, and M. Plapp, *Phys. Rev. B* **78**, 184110 (2008).
- [17] M. Mendeleev, S. Han, D. Srolovitz, G. Ackland, D. Sun, and M. Asta, *Philos. Mag.* **83**, 3977 (2003), potential 2.
- [18] J. H. van der Merwe, *Proc. Phys. Soc. London, Sect. A* **63**, 616 (1950).
- [19] N. A. Gjostein and F. N. Rhines, *Acta Metall.* **7**, 319 (1959).
- [20] K. R. Elder, M. Katakowski, M. Haataja, and M. Grant, *Phys. Rev. Lett.* **88**, 245701 (2002).
- [21] K.-A. Wu and A. Karma, *Phys. Rev. B* **76**, 184107 (2007).
- [22] S. M. Foiles, *Scripta Mater.* **62**, 231 (2010).
- [23] P. Keblinski, D. Wolf, S. Phillpot, and H. Gleiter, *Philos. Mag. A* **79**, 2735 (1999).
- [24] A. Suzuki and Y. Mishin, *J. Mater. Sci.* **40**, 3155 (2005).
- [25] T. Frolov and Y. Mishin, *Phys. Rev. B* **79**, 174110 (2009).